Mapping snow cover in the pan-Arctic zone, using multi-year (1998-2001) images from optical VEGETATION sensor

Xiangming Xiao, Qingyuan Zhang, Stephen Boles, Michael Rawlins, and Berrien Moore III

Institute for the Study of Earth, Oceans and Space, University of New Hampshire, Durham, NH 03833, USA.

Corresponding Author

Xiangming Xiao

Institute for the Study of Earth, Oceans and Space

University of New Hampshire

Durham, NH 03824, USA.

Telephone: (603) 8623818

Fax: (603) 862-0188

Email: xiangming.xiao@unh.edu

International Journal of Remote Sensing

Accepted for publication on May 3, 2004

Short title: snow cover dynamics in the pan-Arctic zone

ABSTRACT

Timely information on spatial distribution and temporal dynamics of snow cover in the pan-Arctic zone is needed, as snow cover plays an important role in climate, hydrology and ecological processes. Here we report estimates of snow cover in the pan-Arctic zone (north of 45^{o}N) at 1-km spatial resolution and at a 10-day temporal interval over the period of 4/1998 – 12/2001, using 10-day composite images of VEGETATION sensor onboard SPOT-4 satellite. The results show that snow covered area (SCA) in North America (north of 45^{o}N) increased from 1998 to 2001, while SCA in Eurasia (north of 45^{o}N) decreased from 1998 to 2000 but increased in 2001. There were large spatial and temporal variations of snow cover in the pan-Arctic zone during 1998-2001.

1. INTRODUCTION

During winter and spring, the land surface in high altitudes, northern temperate and boreal zones are frequently covered by snow. Snow cover is characterized by rapid seasonal changes and large spatial variations, and plays an important role in climate and water resources (Goodison et al., 1999; Groisman and Davies, 2001; Pielke et al., 2000). Variable snow distribution influences the outcomes of simulations of hydrologic and ecosystem processes. The end-of-winter snow distribution is a crucial input to snowmelt hydrology models, including those used for water-resource management (Hartman et al., 1999; Kane et al., 1991; Martinec and Rango, 1981). The problem of realistically representing seasonal snow in atmospheric, hydrologic, and ecological models is made complex because of the numerous snow-related features that display considerable spatial variability at scales below those resolved by the models. A patchy mosaic of

snow and vegetation caused by redistribution and snowmelt strongly influences the energy fluxes returned to the atmosphere, and the associated feedbacks that accelerate the melt of remaining snow-covered areas (Essery, 1997; Liston, 1999; Liston and Sturn, 1998; Neumann and Marsh, 1998; Shook et al., 1993). Seasonal dynamics of snow cover is related to length and timing of photosynthetic active period of vegetation, and affected net ecosystem exchange of CO_2 between forest ecosystems and the atmosphere (Black et al., 2000; Goulden et al., 1996; Goulden et al., 1998). Snow cover dynamics (accumulation, melting and depletion) have significant implications for atmospheric, hydrologic and ecologic modeling (Liston, 1999).

The linkage between snow cover (one of hydrological processes) and biogeochemical processes (CO_2 fluxes and trace gases emissions) takes place at ecosystem to landscape scales. Quantification of CO_2 fluxes and trace gases emissions of terrestrial ecosystems in the pan-Arctic zone has been hampered by lack of geospatial datasets of snow cover at ecosystem- to landscape resolutions (a spatial resolution of a few hundreds of meter to kilometer). At large spatial scales, snow cover detection methods and available snow cover products are primarily based on three groups of space-borne sensors (Chang et al., 1987; Cline and Carroll, 1999; Grody and Basist, 1996; Rango, 1993; Tait et al., 2000): (1) optical sensors (e.g., AVHRR), (2) passive microwave sensors (e.g., DMSP SSM/I, Nimbus-7 SSMR) and (3) active synthetic aperture radar (e.g., Radarsat, ERS-1/2). To date, large-scale (continental to global) operational mapping and monitoring of snow cover has been largely dependent upon the image data from AVHRR onboard the NOAA meteorological satellites (Frei and Robinson, 1999; Robinson et al., 1993). The widely-used Northern Hemisphere EASE-Grid Snow Cover Dataset at National Snow and Ice Data Center (NSIDC, (Armstrong and Brodzik, 2002), (http://nsidc.org/) have a

coarse spatial resolution (e.g., 25-km grid). Satellite and land surface observations have indicated that snow cover area in the Northern Hemisphere has declined significantly over the last several decades, particularly in the spring season (Brown, 2000; Easterling et al., 2000; Groisman et al., 1994b; Robinson et al., 1995).

Recently, a new generation of advanced optical space-borne sensors has successfully been launched (e.g., VEGETATION (VGT) sensor onboard SPOT-4 in 1998, MODIS sensor onboard EOS Terra in 1999). These new sensors have more spectral bands (Table 1) and offer much improved potential for quantifying seasonal dynamics and interannual variation of snow cover in the globe at moderate spatial resolutions (e.g., 500-m to 1-km). In order to reduce data volume and have cloud-free images, 10-day composites of VGT images (http://free.vgt.vito.be) and 8-day composites of MODIS images (http://edc.usgs.gov/products/satellite.html) are provided to users for satellite-based studies of land cover classification, vegetation growth, and CO_2 fluxes. Information on snow cover is needed for analysis of those 10-day composites of VGT images and 8-day composites of MODIS images. Recently, significant progress has been made in using images from those advanced optical sensors (VGT, MODIS) for identifying and mapping of snow cover at such a spatial resolution that is comparable with the studies of ecosystems and landscape processes (Hall et al., 2002; Xiao et al., 2002b). In this study, our specific objective is twofold: (1) to develop a multi-year dataset of snow cover at 1-km spatial resolution over the period of 4/1998 to 12/2001, using the 10-day composites of VGT (VGT-S10) image data; and (2) to further document the potential of VGT sensor for identification and mapping of snow cover at large spatial scales. The resultant snow cover dataset will help quantify seasonal dynamics and interannual variations of snow cover in the pan-Arctic zone from 4/1998 to

12/2001, and could also be used to support other analyses of 10-day composites of VGT images, for instance, forest classification and vegetation indices (Xiao et al., 2002a; Xiao et al., 2003).

2. DATA AND METHODS

2. 1. Multi-temporal images from the VEGETATION (VGT) sensor

The VGT instrument has four spectral bands (Table 1). The blue band is primarily used for atmospheric correction. The SWIR band is sensitive to soil moisture, vegetation cover and leaf moisture content, and can improve the discrimination of vegetation and other land covers. With a swath width of 2,250 km, VGT provides daily coverage of the globe at 1-km spatial resolution. Multi-year VGT images have been accumulated since 4/1998. The VGT sensor uses the same geometric reference system and has identical spectral bands as the SPOT High Resolution Visible and Infrared sensor to facilitate multi-scale interpretation.

Three standard VGT products are available to users: VGT-P (Physical product), VGT-S1 (daily synthesis product) and VGT-S10 (10-day synthesis product). The spectral bands in the VGT-S1 products are estimates of ground surface reflectance, as atmospheric corrections for ozone, aerosols and water vapor have been applied to the VGT-P images using the simplified method for atmospheric correction algorithm (Rahman and Dedieu, 1994). VGT-S10 data are generated by selecting the VGT-S1 pixels that have the maximum Normalized Difference Vegetation Index (NDVI) values within a 10-day period, thus minimizing the effect of cloud cover and variability in atmospheric optical depth. There are three 10-day composites for one month: days 1-10, days 11-20, and day 21 to the last day of a month. Global VGT-S10 data are freely available to the public (http://free.vgt.vito.be). The spatial domain of the global VGT-S10 data ranges from 56^{o}S

to 75^{o}N, which results in a data void region around the North Pole throughout a year. In addition, VGT sensor had no observations at very high latitudes in late-fall/winter/early-spring seasons, because of no sunlight illumination at local passing times of satellite. The resultant data void region (for VGT-S10 data) varied in size over time and thus has some implications on estimates of snow cover area during late-fall/winter/early-spring seasons in the pan-Arctic zone. The maximum snow cover area in early spring season (March) could be used as an approximate estimate of maximum snow cover area in a year, because air temperature in that period (March) could be still too cold for snow cover at very high latitudes to melt.

2.2. Description of the algorithms for identifying snow cover

Snow and ice cover have very high spectral reflectance values in the visible wavelengths (400 - 700 nm), but have low reflectance values in the shortwave infrared wavelengths (1550 - 1750 nm). Among the four types of snow and ice cover with different grain sizes, the differences in spectral reflectance are relatively small in visible wavelengths but large in shortwave infrared wavelengths (Figure 1). The Normalized Difference Snow Index (NDSI), which is calculated as a normalized difference between the spectral reflectance values of green and shortwave infrared bands, was proposed to identify and map snow cover (Hall et al., 1998; Hall et al., 1995). For Landsat TM data, NDSI is calculated using the green band (TM2) and shortwave infrared band (TM5):

$$NDSI_{TM} = (TM2 - TM5) / (TM2 + TM5) \quad (1)$$

Hall et al. (1995, 1998) used NDSI threshold values for snow cover mapping. If a pixel had NDSI $\geq$ 0.40 and near-infrared (NIR) reflectance >0.11, the pixel was classified as snow/ice

cover. This NDSI-based algorithm (SNOMAP) is used to generate the MODIS standard product for snow cover at the global scale (Hall et al., 1995; Hall et al., 2002).

Other studies have suggested that red wavelengths are useful for identifying snow and ice cover (Boresjo Bonge and Bronge, 1999; Sidjak and Wheate, 1999). Using Landsat TM data and ground radiometer measurements to classify ice and snow-type in the eastern Antarctic, *Boresjö Bronge and Bronge* (1999) found that the RED/NIR (TM3/TM4) ratio is a simple tool for distinguishing between blue-ice and snow, and the RED/SWIR (TM3/TM5) ratio is a useful tool for quantifying snow grain-size variations. The Normalized Difference Snow/Ice Index (NDSII), which is calculated as a normalized difference between red and shortwave infrared bands, was proposed (Xiao et al., 2001). For Landsat TM data, NDSII is calculated as:

$$NDSII_{TM} = (TM3 - TM5)/(TM3 + TM5) \quad (2)$$

A comparison study of NDSI and NDSII was conducted, using one Landsat TM image in the Qinghai-Tibet plateau of China (Xiao et al., 2001). Spatial data of NDSI and NDSII from the Landsat TM image showed that NDSII values were highly correlated with NDSI values. To determine whether a pixel is covered by snow/ice or not, the same thresholds proposed by *Hall et al*. (1995, 1998) were used. If a pixel had NDSII $\geq$ 0.40 or NDSI $\geq$ 0.40 and a NIR reflectance value >0.11, the pixel was classified as snow/ice. The results showed that the NDSI- and NDSII-based algorithms gave similar estimates of area and spatial distribution of snow/ice cover (Xiao et al., 2001). Because the VGT sensor has red and shortwave infrared bands equivalent to Landsat TM (Table 1), it has the potential for identifying and mapping snow cover at large spatial scales. For VGT data, NDSII is calculated using surface reflectance values of red (B2) and shortwave infrared (SWIR) bands:

$$NDSII_{VGT} = (RED - SWIR)/(RED + SWIR) \quad (3)$$

The VGT-specific $NDSII_{vgt}$ (Equation 3) was first used to identify and map snow/ice cover in the Qinghai-Tibet Plateau of China, using 10-day composite VGT data from March 1999 to November 1999 (Xiao et al., 2002b). Using the snow/ice identification thresholds (NDSII $\geq$ 0.40 and NIR >0.11) developed in earlier study (Xiao et al., 2001), the VGT NDSII algorithm provided reasonable estimates of the spatial and temporal dynamics of snow/ice cover in the entire Qinghai-Tibet Plateau (Xiao et al., 2002b).

In this study, we downloaded VGT-S10 data for North America, Europe and North Asia over the period of April 1-10, 1998 to December 21-31, 2001 (a total of 135 observations in the time series data at 10-day interval). The data of these three regions were combined together and subset to cover the pan-Arctic zone (north of 45^{o}N to 75^{o}N). Note that as sun illumination in high latitudes changes over seasons, the land area that is observed by optical VGT sensor also changes accordingly, with the least amount of observations in winter season and the largest amount of observations in summer season in the pan-Arctic zone. We first calculated $NDSII_{VGT}$ for all the VGT-S10 composites during 4/1998 – 12/2001, and then applied the same decision thresholds (NDSII $\geq$ 0.40 and NIR >0.11) used in the earlier studies (Xiao et al., 2002b; Xiao et al., 2001) to identify and map snow cover. The VGT-S10 product provides cloud flag in status map file, and we excluded those cloudy pixels in calculation of $NDSII_{VGT}$ and snow cover.

3. RESULTS

There were distinct seasonal dynamics of snow-covered area (SCA) in the pan-Arctic zone (Figure 2a). Conventional definitions of the four seasons are used here: winter (December,

January, February), spring (March, April, May), summer (June, July, August) and fall (September, October, November). During mid-summer, SCA reached its lowest values within a year. SCA increased gradually from late September, as the fall and winter seasons approach. SCA was generally highest during late winter and early spring. As the spring season progresses, air temperature increased and SCA declined gradually. While the seasonality of SCA in North America (Figure 2c) is generally similar to that in Eurasia (Figure 2b), snowmelt tends to occur slightly earlier in Eurasia than in North America in the spring (Figure 2b,c).

There were only slight interannual variations of SCA for the pan-Arctic zone during 1998-2001 (Figure 2a). SCA in the pan-Arctic zone increased in late spring during 1998-2001 but decreased in fall during 1998-2000. Spring and fall seasons of year 2001 had the largest SCA in the pan-Arctic zone. Geographically, interannual variation of SCA differed between North America and Eurasia (Figure 2b, c). The SCA in North America (north of 45^{o}N) increased slightly from 1998 to 2001, in both late spring to early summer and fall season (Figure 2b). In contrast, SCA in Eurasia had a slight decrease from 1998 to 2001 in spring season, and a relatively large decline from 1998 to 2000 in fall season (Figure 2c). The SCA in Eurasia was higher in fall of 2001 than the other three years.

We calculated SCA frequency (number of observations as snow cover within a year) for individual image pixels and generated maps to illustrate the spatial distribution of snow cover (Figure 3). In general, the spatial distributions of SCA frequency agreed relatively well among years (1998-2001). The large SCA in Eurasia in 2001 (Figure 2c) was mostly attributed to more snow cover in eastern part of Eurasia, including Mongolian Plateau and the northeastern part of

the Far East of Russia (Figure 3). The high SCA frequency occurred in mountains (e.g., Rocky Mountains in western North America). The spatial distribution of snow/ice cover was strongly influenced by topography (Cline, 1997; Cline et al., 1998; Konig and Sturn, 1998). We downloaded the Global Land One-kilometer Base Elevation (GLOBE) digital elevation data set, which was released by the NOAA National Geophysical Data Center (NDGC) in 1999 (the website http://www.ngdc.noaa.gov/). The digital elevation model (DEM) dataset has a spatial resolution of 30 arc second (Figure 4). The DEM dataset for the pan-Arctic zone was co-registered with the VGT-derived snow cover dataset. Visual comparison of the DEM and the snow cover datasets revealed a strong spatial agreement between snow cover and topographical features (Figure 3, 4).

4. DISCUSSIONS

The resultant multi-year VGT snow cover dataset will supplement other existing multi-year snow cover datasets, such as those derived from AVHRR images (Armstrong and Brodzik, 2002; Cline and Carroll, 1999; Ramsay, 1998). A simple comparison between the VGT snow cover dataset and the Northern Hemisphere EASE-Grid Snow Cover dataset (Armstrong and Brodzik, 2002) archived at the National Snow and Ice Data Center (The snow cover dataset was called as NSIDC version 2 in this study) was conducted (Figure 5). For the NSIDC Version 2 snow cover dataset (10/3/1966 – 6/24/2001), snow cover extent is based on the digital NOAA-NESDIS Weekly Northern Hemisphere Snow Charts, revised by D. Robinson (Rutgers University) and regridded to the EASE-Grid (25-km equal-area grid). The original NOAA-NESDIS weekly snow charts are derived from the manual interpretation of AVHRR, GOES, and other visible-band satellite data (Armstrong and Brodzik, 2002). The 1-km VGT-derived snow cover data were

aggregated to 25-km EASE grid. While the seasonal dynamics of snow cover were similar, the total SCA between the VGT dataset and NSIDC Version 2 dataset differed significantly over seasons, particularly in winter. The differences in total SCA could be attributed to a few sources. First of all, as shown in Figure 6, there are some differences in spatial coverage between the VGT-S10 reflectance dataset (only reaching 75^{o}N during summer) and the NSIDC Version 2 dataset (covering the entire Arctic circle). Secondly, the VGT-S10 reflectance data had no observations for very high latitudes during the winter season because of no sunlight illumination, it resulted in under-estimation of snow cover area during winter and early spring seasons. Thirdly, the NSIDC version 2 snow cover dataset is a binary map (presence or no presence map) at 25-km grid. If a gridcell was assigned as snow cover, the entire gridcell area (25×25 km^2) is assumed to be snow cover, without considering actual percentage fraction of snow cover within the gridcell (ranging from 50% to 100%), which is likely to result in overestimation of snow cover area. In contrast, the VGT-derived snow cover dataset has a spatial resolution of 1-km, and is aggregated to calculate percentage fraction of snow cover within individual EASE-Grid cells (25-km spatial resolution). Fourthly, since the 10-day composites of VGT data were used in this study, it is likely that the compositing method used in generating 10-day composites (selecting an observation of maximum NDVI value within a 10-day period) might miss some short-duration (less than 10-days) snow events, particularly in late spring and early fall seasons, when land surface temperature is warm and snow may melt within a few days. There also existed some differences in spatial distribution of snow cover between the NSIDC Version 2 snow cover dataset and the VGT-derived snow cover dataset, for instance, during the early April 2000, snow covered area in the VGT-derived snow cover dataset was much less than the NSIDC snow cover dataset in southern part of the pan-Arctic zone (Figure 6), when using the threshold of ≥50%

snow cover within individual EASE-Grid cells, which was used in generating the NSIDC Northern Hemisphere Weekly EASE-Grid snow cover dataset (Armstrong and Brodzik, 2002).

A number of studies have indicated that there is a strong linkage between Eurasian snow cover and climate (Clark et al., 1999; Cohen and Entekhabi, 1999; Douville and Royer, 1996). North Atlantic Oscillation (NAO) is the primary control factor for winter climate variability in the North Atlantic region ranging from central North America to Europe and much into Northern Asia. The positive (or negative) NAO index phases were closely related to winter climate and varied over years (Hurrell, 1995). Year 1998, 1999 and 2000 had positive NAO index, while year 2001 had negative NAO index. In those years with positive NAO index, Europe had warm and wet winters, but northern Canada and Greenland had cold and dry winter, and the eastern US experienced mild and wet winter conditions. In those years with negative NAO index, the US east coast experienced more cold air outbreaks and hence snowy weather condition (http://www.cgd.ucar.edu/~jhurrell/nao.html). Snow cover affected heat balance and spring temperature at continental scale (Groisman and Davies, 2001; Groisman et al., 1994a). Therefore, observed variations of snow cover during 1998-2001 in the pan-Arctic zone (Figure 3) may have impacts on climate in Eurasia and North America.

It is important to note that the one of major advantages of VGT-derived snow cover dataset is the spatial resolution (1-km), in comparison with other coarse resolution snow cover datasets (e.g., NSIDC Northern Hemisphere Weekly EASE-Grid snow cover dataset (Armstrong and Brodzik, 2002)), as analyses of the linkage between hydrological process (e.g., snow cover) and biogeochemical process(e.g., CO_2 fluxes) of terrestrial ecosystems require temporally and

spatially consistent dataset resolved at such a spatial resolution (e.g., hundreds of meters to km) that is closely relevant to ecosystem and landscape processes. Earlier studies (Xiao et al., 2002b; Xiao et al., 2001) and this study have demonstrated the potential of optical VGT sensor for identification and mapping of snow cover at large spatial scales. As more VGT images are available in the near future (from VGT sensors onboard SPOT-4 satellite and SPOT-5 satellite), the multi-year VGT-based dataset of snow cover at 1-km spatial resolution and 10-day temporal resolution is likely to improve simulations of climate, hydrological and ecological processes in the pan-Arctic zone.

ACKNOWLEDGEMENTS

This study was supported by the NASA Earth Observing System (EOS) Interdisciplinary Science (IDS) program (NAG5-6137, NAG5-10135). We thank anonymous reviewers for their comments and suggestions on the earlier version of the manuscript.

REFERENCES

Armstrong, R.L. and Brodzik, M.J., 2002. Northern Hemisphere EASE-Grid weekly snow cover and sea ice extent version 2. National Snow and Ice Data Center, Boulder, Colorado, USA.

Black, T.A. et al., 2000. Increased carbon sequestration by a boreal deciduous forest in years with a warm spring. Geophysical Research Letters, 27: 1271-1274.

Boresjo Bonge, L.B. and Bronge, C., 1999. Ice and snow-type classification in the Vestfold Hill, East Antarctic, using Landsat TM data and ground radiometer measurements. International Journal of Remote Sensing, 20: 225-240.

Brown, R.D., 2000. Northern Hemisphere snow cover variability and change: 1915-97. Journal of Climate, 13: 2339-2355.

Chang, A., Foster, J.L. and Hall, D.K., 1987. Nimbus-07 SMMR derived global snow cover parameters. Annuals of Glaciology, 9: 39-44.

Clark, M.P., Serreze, M.C. and Robinson, D.A., 1999. Atmospheric controls on Eurasian snow extent. International Journal of Climatology, 19: 27-40.

Cline, D.W., 1997. Effects of seasonality of snow accumulation and melt on snow surface energy exchanges at a continental alpine site. Journal of Applied Meteorology, 36: 32-51.

Cline, D.W., Bales, R.C. and Dozier, J., 1998. Estimating the spatial distribution of snow in mount basins using remote sensing and energy balance modeling. Water Resources Research, 34: 1275-1285.

Cline, D.W. and Carroll, T.R., 1999. Operational automated production of daily, high-resolution, cloud-free snow cover maps of the continental U.S. Journal of Geophysical Research-Atmospheres, 104(D16): 19631-19644.

Cohen, J. and Entekhabi, D., 1999. Eurasian snow cover variability and Northern Hemisphere climate predictability. Geophysical Research Letters, 26(3): 345-348.

Douville, H. and Royer, J.F., 1996. Sensitivity of the Asian summer monsoon to an anomalous Eurasian snow cover within the Meteo-France GCM. Climate Dynamics, 12: 449-466.

Easterling, D.R. et al., 2000. Observed climate variability and change of relevance to the biosphere. Journal of Geophysical Research-Atmospheres, 105: 20101-20114.

Essery, R.L., 1997. Modeling fluxes of momentum, sensible heat and latent heat over heterogenous snow cover. Quarterly Journal of The Royal Meteorological Society, 123: 1867-1883.

Frei, A. and Robinson, D.A., 1999. Northern Hemisphere snow extent: regional variability 1972-1994. International Journal of Climatology, 19: 1535-1560.

Goodison, B.E., Brown, R.D. and Crane, R.G., 1999. Cryospheric systems. In: M.D. King (Editor), EOS Science Plan: The State of Science in the EOS Program. NASA, pp. 261-307.

Goulden, M.L., Munger, J.W., Fan, S.M., Daube, B.C. and Wofsy, S.C., 1996. Exchange of carbon dioxide by a deciduous forest: Response to interannual climate variability. Science, 271(5255): 1576-1578.

Goulden, M.L. et al., 1998. Sensitivity of boreal forest carbon balance to soil thaw. Science, 279(5348): 214-217.

Grody, N.C. and Basist, A.N., 1996. Global identification of snow cover using SSM/I measurements. IEEE Transactions on Geoscience and Remote Sensing, 34: 237-249.

Groisman, P.Y. and Davies, T.D., 2001. Snow cover and the climate system. In: J.G. Jones, J.W. Pomeroy, D.A. Walker and R.W. Hoham (Editors), Snow Ecology. Cambridge University Press, New York, pp. 1-44.

Groisman, P.Y., Karl, T.R. and Knight, R.W., 1994a. Observed impact of snow cover on the heat balance and the rise of continental spring temperature. Science, 263: 198-200.

Groisman, P.Y., Karl, T.R., Knight, R.W. and Stenchiko, G.L., 1994b. Change of snow cover, temperature, and radiative heat balance over the Northern Hemisphere. Journal of Climate, 7: 1633-1656.

Hall, D.K., Foster, J.L., Verbyla, D.L. and Klein, A.G., 1998. Assessment of snow cover mapping accuracy in a variety of vegetation cover densities in central Alaska. Remote Sensing of Environment, 66: 129-137.

Hall, D.K., Riggs, G.A. and Salomonson, V.V., 1995. Development of methods for mapping global snow cover using moderate resolution imaging spectroradiometer data. Remote Sensing of Environment, 54: 127-140.

Hall, D.K., Riggs, G.A., Salomonson, V.V., DiGirolamo, N.E. and Bayr, K.J., 2002. MODIS snow-cover products. Remote Sensing of Environment, 83: 181-194.

Hartman, M.D. et al., 1999. Simulations of snow distribution and hydrology in a mountain basin. Water Resources Research, 35: 1587-1603.

Hurrell, J.W., 1995. Decadal trends in the North Atlantic Oscillation: Regional temperature and precipitation. Science, 269: 676-679.

Kane, D.L., Hinzman, L.D., Benson, C.S. and Liston, G.E., 1991. Snow hydrology of a headwater Arctic basin 1. Physical measurement and process studies. Water Resources Research, 27: 1099-1109.

Konig, M. and Sturn, M., 1998. Mapping snow distribution in the Alaskan Arctic using air photos and topographic relationships. Water Resources Research, 34: 3471-3483.

Liston, G.E., 1999. Interrelationships among snow distribution, snowmelt, and snow cover depletion: Implications for atmospheric, hydrologic, and ecologic modeling. Journal of Applied Meteorology, 38(10): 1474-1487.

Liston, G.E. and Sturn, M., 1998. A snow transport model for complex terrain. Journal of Glaciology, 44(148): 498-516.

Martinec, J. and Rango, A., 1981. Areal distribution of snow water equivalent evaluated by snow cover monitoring. Water Resources Research, 17: 1480-1488.

Neumann, N. and Marsh, P., 1998. Local advection of sensible heat in the snowmelt landscape of Arctic tundra. Hydrological Processes, 12: 1547-1560.

Pielke, R.A., Liston, G.E. and Robock, A., 2000. Insolation-weighted assessment of Northern Hemisphere snow cover and sea-ice variability. Geophysical Research Letters, 27: 3061-3064.

Rahman, H. and Dedieu, G., 1994. SMAC: A simplified method for atmospheric correction of satellite measurements in the solar spectrum. International Journal of Remote Sensing, 15: 123-143.

Ramsay, B., 1998. The interactive multisensor snow and ice mapping system. Hydrological Processes, 12: 1537-1546.

Rango, A., 1993. Snow hydrology processes and remote sensing. Hydrological Processes, 7: 121-138.

Robinson, D.A., Dewey, K.F. and Heim, R.R., 1993. Global snow cover monitoring:An update. Bulletin of the American Meteorological Society, 74: 1689-1696.

Robinson, D.A., Frei, A. and Serreze, M.C., 1995. Recent variations and regional relationships in Northern Hemisphere snow cover. Annuals of Glaciology, 21: 71-76.

Shook, K., Gray, D.M. and Pomeroy, J.W., 1993. Temporal variation in snow cover area during snowmelt in prairie and alpine environments. Nordic Hydrology, 24: 183-198.

Sidjak, R.W. and Wheate, R.D., 1999. Glacier mapping of the Illecillewaet icefield, British Columbia, Canada ,using Landsat TM and digital elevation data. International Journal of Remote Sensing, 20: 273-284.

Tait, A.B., Hall, D.K., Foster, J.L. and Armstrong, R.L., 2000. Utilizing multiple datasets for snow-cover mapping. Remote Sensing of Environment, 72: 111-126.

Xiao, X., Boles, S., Liu, J.Y., Zhuang, D.F. and Liu, M.L., 2002a. Characterization of forest types in Northeastern China, using multi-temporal SPOT-4 VEGETATION sensor data. Remote Sensing of Environment, 82(2-3): 335-348.

Xiao, X. et al., 2003. Sensitivity of vegetation indices to atmospheric aerosols: continental-scale observations in Northern Asia. Remote Sensing of Environment, 84(3): 385-392.

Xiao, X., Moore, B., Qin, X., Shen, Z. and Boles, S., 2002b. Large-scale observations of alpine snow and ice cover in Asia: Using multi-temporal VEGETATION sensor data. International Journal of Remote Sensing, 23(11): 2213-2228.

Xiao, X.M., Shen, Z.X. and Qin, X.G., 2001. Assessing the potential of VEGETATION sensor data for mapping snow and ice cover: a Normalized Difference Snow and Ice Index. International Journal of Remote Sensing, 22(13): 2479-2487.

Table 1. A comparison of spectral bands among SPOT-4 (VGT), NOAA AVHRR, Terra MODIS and Landsat TM optical sensors

Feature	**SPOT-4 VGT**	**NOAA AVHRR**	**Terra MODIS**	**Landsat TM**
Blue	B0 (430 - 470)		B3 (459 – 479)	TM1 (450 – 520)
Green			B4 (545 – 565)	TM2 (520 – 600)
Red	B2 (610 - 680)	CH1 (580 - 680)	B1 (620 – 670)*	TM3 (630 – 690)
Near infrared	B3 (780 - 890)	CH2 (725 – 1100)	B2 (841 – 876)*	TM4 (760 – 900)
			B5 (1230 – 1250)	
Shortwave infrared	SWIR (1580 – 1750)		B6 (1628 – 1652)	TM5 (1550 – 1750)
			B7 (2105 – 2155)	TM7 (2080 – 2350)
Spatial resolution	1-km	1-km	250-m*, 500-m	30-m
Revisit time	daily	Daily	Daily	16-day

Figure legend

Figure 1. Spectral reflectance of four types of snow and ice cover, as measured according to Landsat 5 TM spectral bandwidth. It is based upon the spectral library for snow and ice covers from the Johns Hopkins University. The spectral library and spectral re-sampling algorithm are available in the commercial ENVI software (Research System Inc.), and we conducted spectral re-sampling of the spectral library, using Landsat 5 TM spectral bandwidth.

Figure 2. Seasonal dynamics and interannual variations of snow cover in the pan-Arctic zone (45^{o}N to 72^{o}N) during 4/1998 – 12/2001. (a) SCA in the pan-Arctic zone; (b) SCA in North America, and (c) SCA in Eurasia. Note that there are no observations from optical VGT sensor during winter for large portion of high latitudes because of no sun illumination, SCA was underestimated in winter season. The largest SCA in early spring can be used to estimate SCA in the winter season.

Figure 3. The spatial distribution of snow cover frequency (# of observations as snow cover within a year) in the pan-Arctic zone (45^{o}N - 72^{o}N). There are thirty-six 10-day composites of VGT images in a year. (a) 1/1 – 12/31, 1999, (b) 1/1 – 12/31, 2000, and (c) 1/1 – 12/31/2001. Note that here we do not include the snow cover frequency map of 1998, as SPOT-4 VGT sensor was launched in March 1998 and VGT-S10 data are available only for the period of 4/1998 – 12/1998.

Figure 4. Digital Elevation Model for the pan-Arctic zone. Elevation ranges from 0 to 3341 meter, as shown in the color legend.

Figure 5. A comparison of total snow covered area (SCA) between the NSIDC Northern Hemisphere Weekly EASE-Grid snow cover dataset (Armstrong and Brodzik, 2002) and the VGT-derived snow cover dataset for the pan-Arctic zone (45^{o}N and poleward).

Figure 6. A comparison of spatial distribution of snow cover between the NSIDC Northern Hemisphere Weekly EASE-Grid snow cover dataset (Armstrong and Brodzik, 2002) and the VGT-derived snow cover dataset for the pan-Arctic zone (45^{o}N and poleward). The 1-km VGT snow cover dataset was aggregated by calculating the percent fraction of snow cover within individual EASE-Grid cells (25-km spatial resolution). Color legend of the graphs is the following: EASE-Grid cells with snow (>= 50 % of grid cell is snow covered) in blue, and without snow (< 50% snow) in gray. Yellow color in the lower panel represents no-data (data void region throughout a year) in the VGT-S10 images.

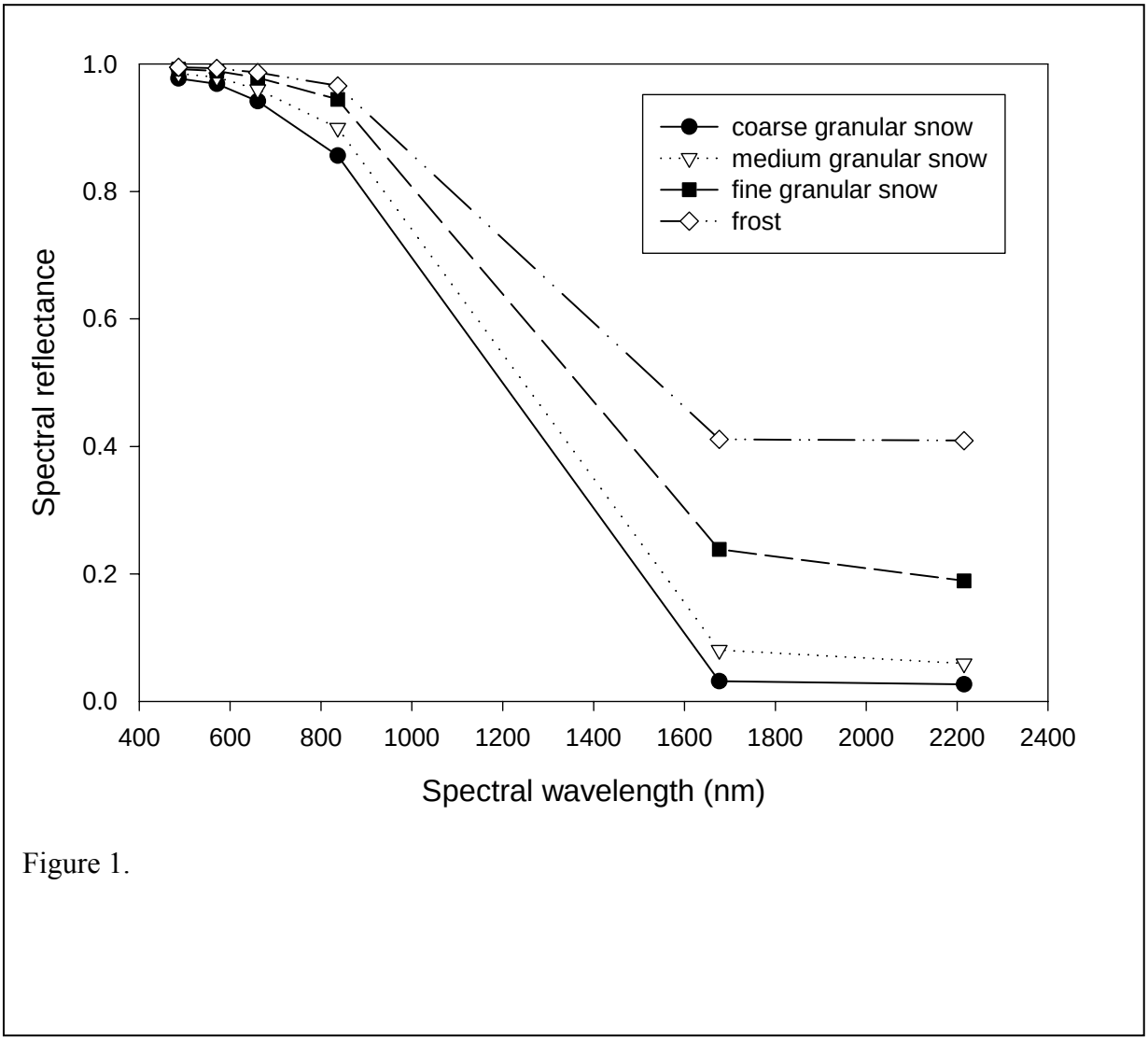
1.0
0.8
0.6
0.4
0.2
0.0
Spectral reflectance
400
600
800
1000
1200
1400
1600
1800
2000
2200
2400
Spectral wavelength (nm)
coarse granular snow
medium granular snow
fine granular snow
frost

Figure 1.

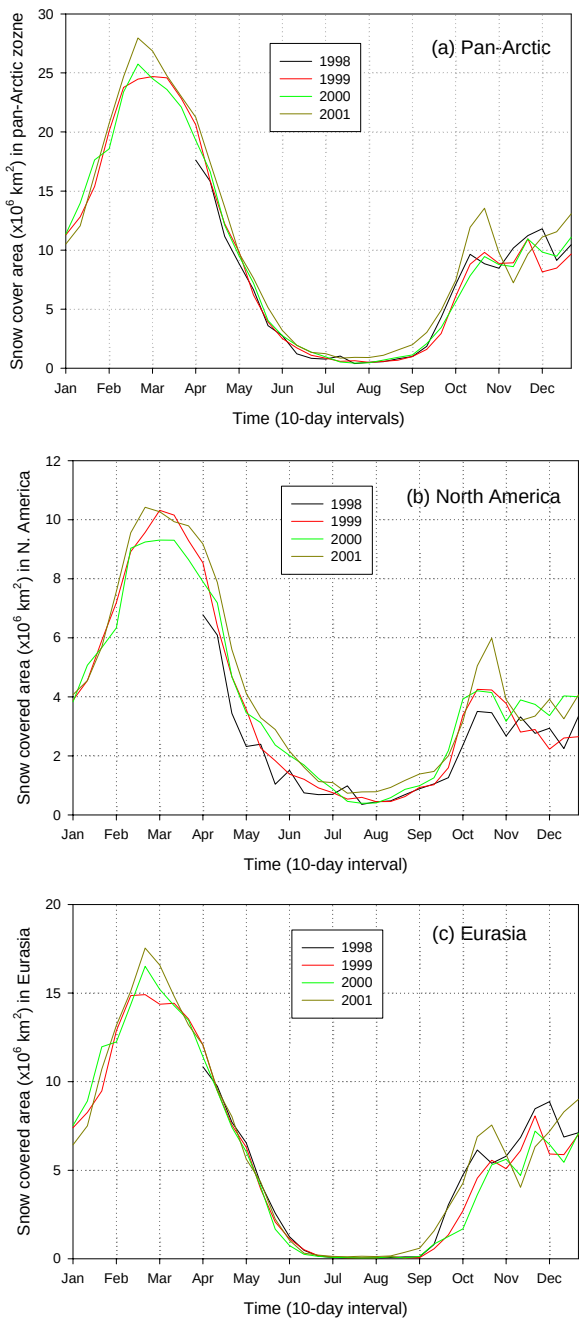
(a) Pan-Arctic
1998
1999
2000
2001
Snow cover area (x10^6 km^2) in pan-Arctic zozne
Time (10-day intervals)
(b) North America
Snow covered area (x10^6 km^2) in N. America
Time (10-day interval)
(c) Eurasia
Snow covered area (x10^6 km^2) in Eurasia
Time (10-day interval)
Jan
Feb
Mar
Apr
May
Jun
Jul
Aug
Sep
Oct
Nov
Dec

Figure 2

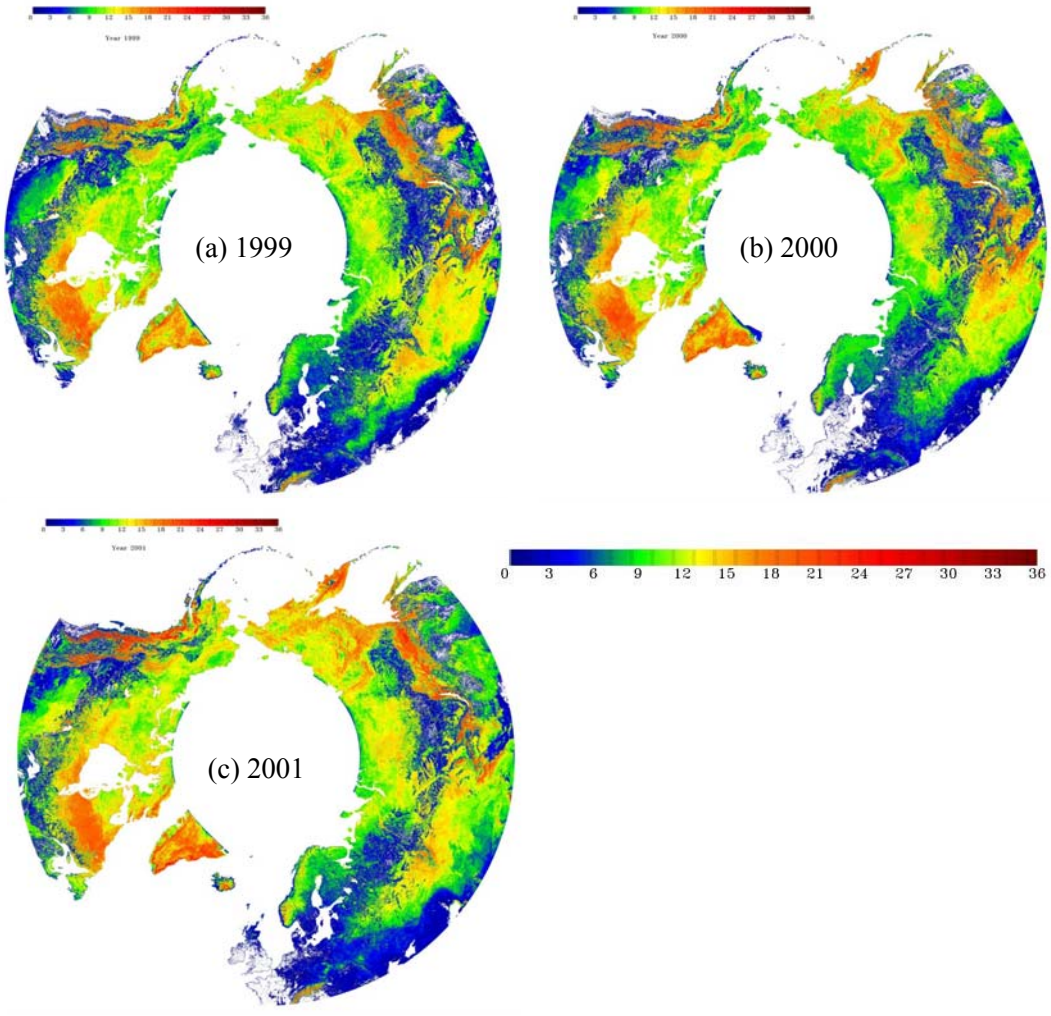

Figure 3.

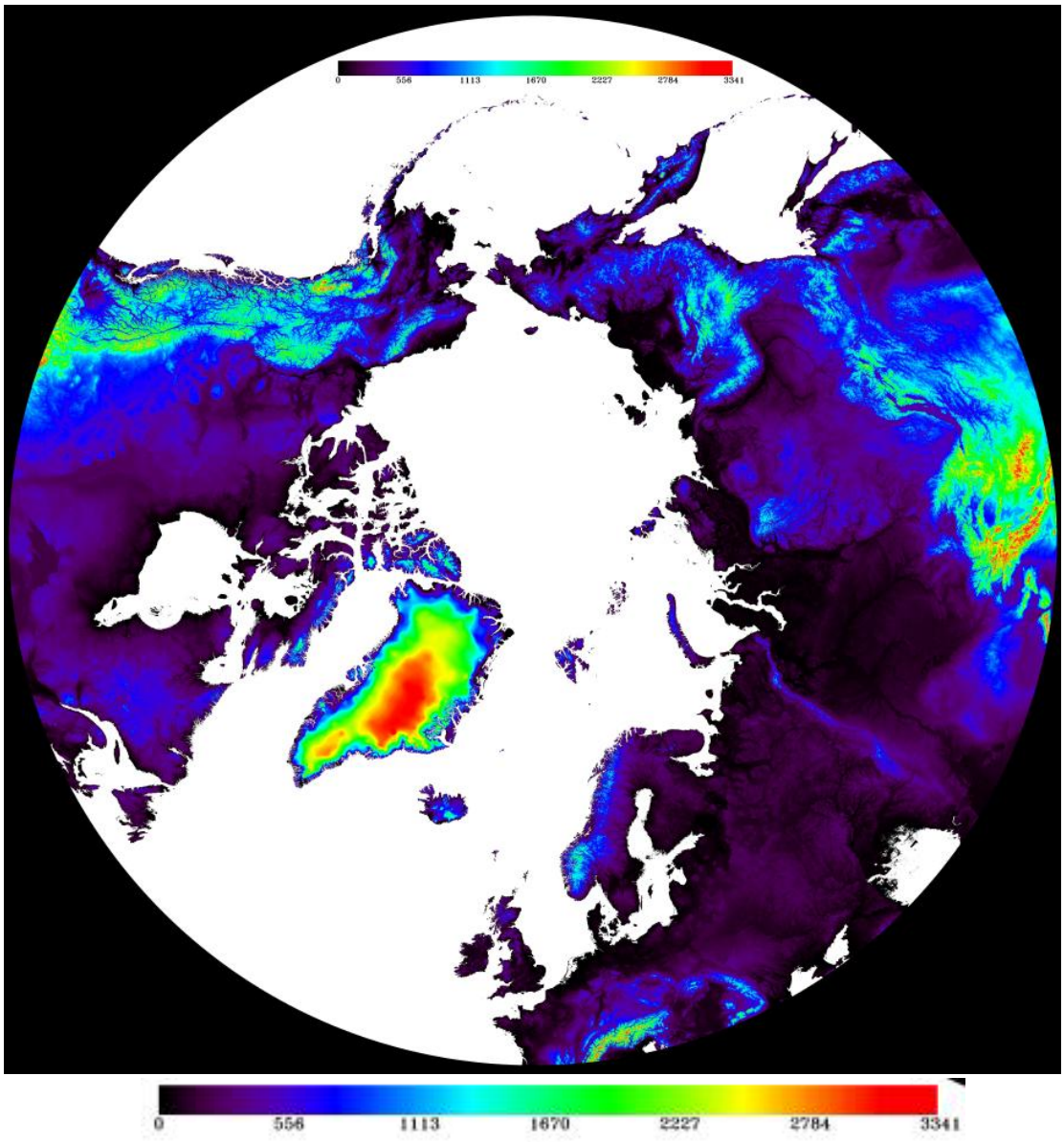

Figure 4

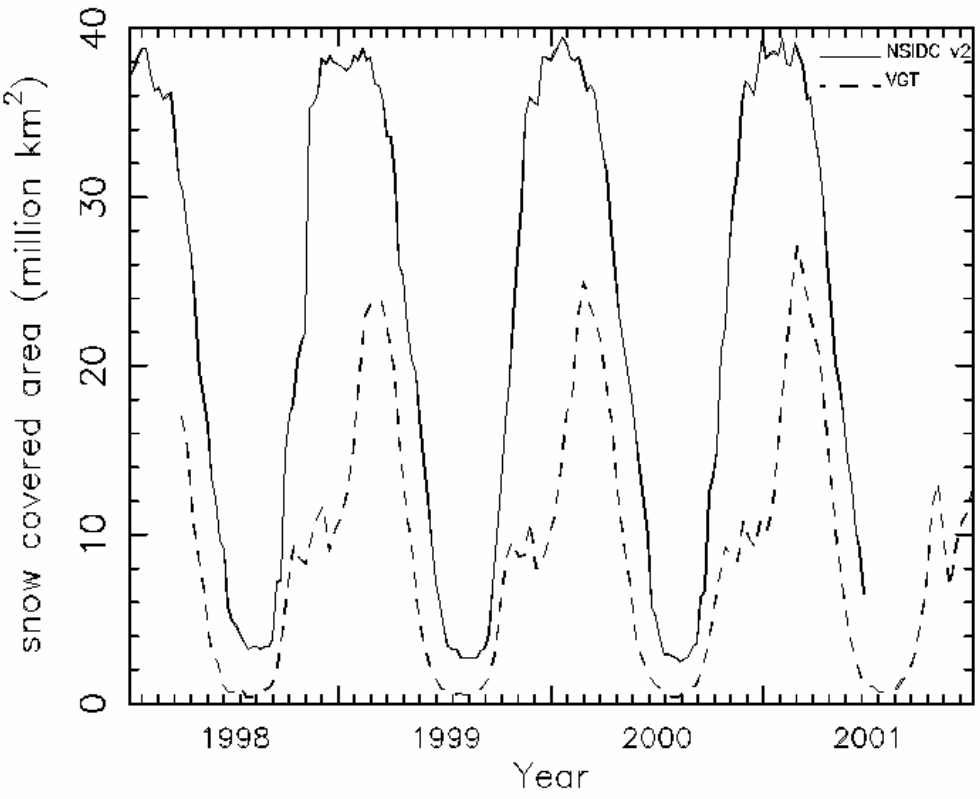
snow covered area (million km^2)
0
10
20
30
40
1998
1999
2000
2001
Year
NSIDC v2
VGT

Figure 5

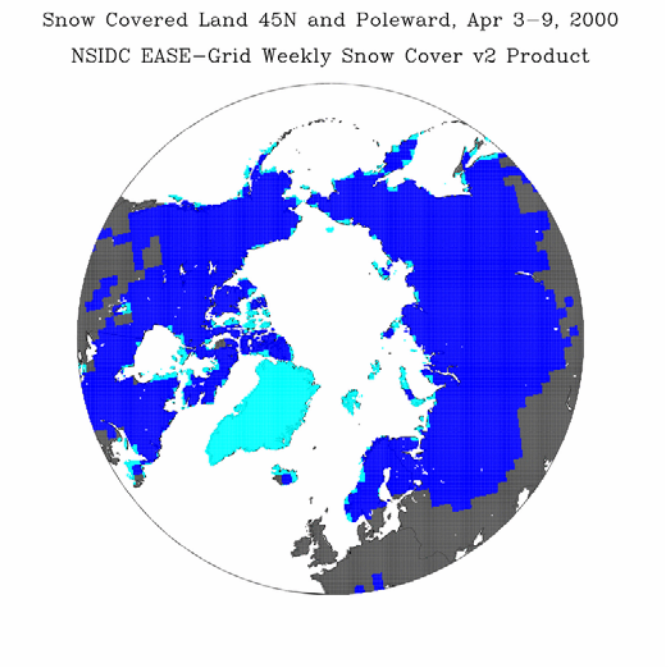
Snow Covered Land 45N and Poleward, Apr 3–9, 2000
NSIDC EASE-Grid Weekly Snow Cover v2 Product

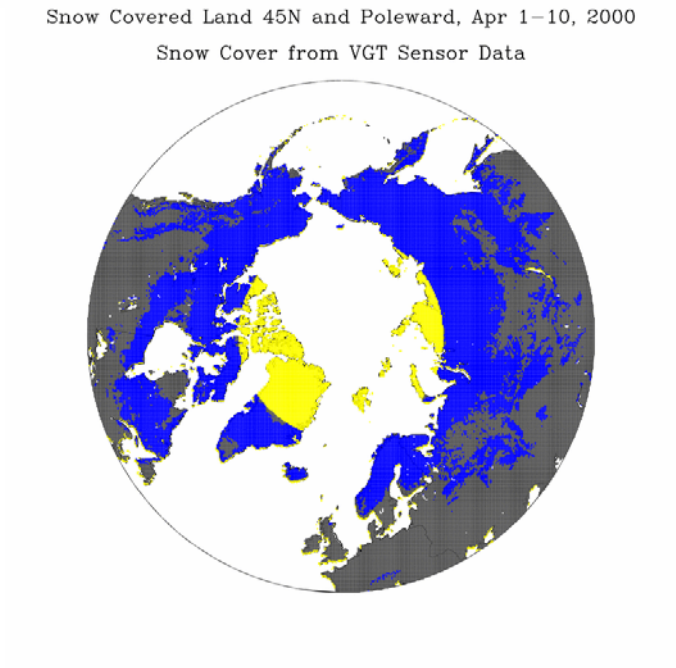
Snow Covered Land 45N and Poleward, Apr 1–10, 2000
Snow Cover from VGT Sensor Data

Figure 6